A structural, magnetic, and Mössbauer spectral study of the TbCo4-xFexB compounds with x=0, 1, and 2

Hervé Mayot, Olivier Isnard, Fernande Grandjean, Gary J. Long

A structural, magnetic, and Mössbauer spectral study of the $TbCo_{4-x}Fe_xB$ compounds with $x=0$, 1, and 2

Hervé Mayot,[1] Olivier Isnard,[1,a)] Fernande Grandjean,[2,b)] and Gary J. Long[3,c)]
[1]*Institut Néel, CNRS and Université de Grenoble Joseph Fourier, Avenue des Martyrs, BP166, F-38000 Grenoble, France*
[2]*Department of Physics, B5, University of Liège, B-4000 Sart-Tilman, Belgium*
[3]*Department of Chemistry, Missouri University of Science and Technology, University of Missouri, Rolla, Missouri 65409-0010, USA*

(Received 14 February 2009; accepted 23 April 2009; published online 2 June 2009)

The $TbCo_{4-x}Fe_xB$ compounds with $x=0$, 1, and 2 have been investigated by x-ray and neutron diffraction, magnetic measurements, and iron-57 Mössbauer spectroscopy. The substitution of cobalt by iron induces both an anisotropic increase in the unit-cell volume and a large increase of approximately 250 K in the Curie temperature; the 4.2 K magnetization decreases continuously with increasing iron content. The powder neutron diffraction patterns and the Mössbauer spectra of the $TbCo_{4-x}Fe_xB$ compounds reveal a strong preferential substitution of iron for cobalt on the 2*c* site, small transition metal magnetic moments of approximately $1.7\mu_B$, and small iron hyperfine fields of approximately 16 T. The compensation temperature of the $TbCo_{4-x}Fe_xB$ compounds decreases continuously from 400 to 350 K between $x=0$ and 2 as the result of an iron induced increase in the transition metal magnetization. The magnetic moment and hyperfine field are found to be larger on the 2*c* site than on the 6*i* site, a difference that reflects the strong hybridization of the 3*d* orbitals of the 6*i* site transition metal with the boron 2*p* orbitals. © *2009 American Institute of Physics*. [DOI: 10.1063/1.3138808]

I. INTRODUCTION

The intermetallic compounds that combine a rare earth, *R*, with a transition metal, *M*, and boron have been intensively investigated over the past 20 years and this work has led to the discovery and better understanding[1] of the properties of $Nd_2Fe_{14}B$, a high performance magnetic material. The interplay of the localized rare-earth 4*f* orbitals, and their associated magnetic moments, with the delocalized transition metal 3*d* orbitals, and their associated magnetic moments, can lead to exceptional magnetic properties. However, the optimization of these properties requires a precise knowledge of the fundamental structural properties of intermetallic compounds. The addition of a ternary component, such as boron or carbon, to an intermetallic binary *RM* compound can lead to a new ternary structure and/or modify the magnetic properties of *R* and *M* in the ternary structure.

The ordered substitution of boron for cobalt in the RCo_5 compounds has been shown to lead to a wide range of $R_{n+1}Co_{3n+5}B_{2n}$ compounds[2,3] that exhibit different crystal structures within the same $P6/mmm$ space group. These compounds are of interest because they are model compounds for probing the influence of metalloid atoms on the magnetic properties of a compound.[4,5]

Herein, we present a crystallographic and magnetic study of the $TbCo_{4-x}Fe_xB$ compounds, with $x=0$, 1, and 2, where the substitution of iron for cobalt is used to modify the magnetic properties of the transition metal sublattice. $TbCo_4B$ is ferrimagnetic below 455 K and exhibits a compensation temperature of 400 K, the temperature at which the terbium and cobalt sublattice magnetizations cancel. The occurrence of this compensation makes such materials[6] useful for both magneto-optical recording and spintronic devices. The series of $TbCo_{4-x}Fe_xB$ compounds has been chosen both because, in contrast to YCo_4B, $TbCo_4B$ does not exhibit a spin reorientation and because the planar magnetic anisotropy of terbium is expected to dominate[7] the magnetocrystalline anisotropy below the Curie temperature. In spite of this dominance, the presence of a cone[8] of easy magnetization at low temperature has, however, been proposed. Hence, it is important to investigate in detail the magnetic behavior of the $TbCo_{4-x}Fe_xB$ compounds and to compare these properties with those obtained for the isotypic $RCo_{4-x}Fe_xB$ compounds.

II. EXPERIMENTAL

The polycrystalline $TbCo_{4-x}Fe_xB$ compounds with $x=0$, 1, and 2 have been prepared by melting starting materials of 99.9% or higher purity in an arc furnace. The ingots were remelted in a high frequency furnace under an argon atmosphere for better homogeneity. Small pieces of the ingots were wrapped in tantalum foil, sealed in an evacuated silica tube, and annealed for 10 days at 1173 K. The phase purity of the samples before and after annealing was determined by powder x-ray diffraction by using copper Cu $K\alpha_1$ 1.5406 Å radiation. $TbCo_3FeB$ contains a small amount of $Tb_3M_{11}B_4$ impurity, where *M* is cobalt and/or iron.

The annealed ingots were powdered and, for the oriented powder x-ray diffraction studies, the particles were sieved to a diameter of less than 0.050 mm. The particles were then

a)Electronic mail: olivier.isnard@grenoble.cnrs.fr.
b)Electronic mail: fgrandjean@ulg.ac.be.
c)Electronic mail: glong@mst.edu.

TABLE I. The 295 K unit-cell parameters, 4.2 K spontaneous magnetizations, and the Curie and compensation temperatures for $TbCo_{4-x}Fe_xB$.

x	a (Å)	c (Å)	V (Å^3)	c/a	M_s (μ_B)	T_C (K)	T_{comp} (K)	T_{comp}/T_C
0[a]	5.038(4)	6.890(8)	151.4(4)	1.368	5.0	455	400	0.88
1	5.073(5)	6.857(8)	152.8(5)	1.351	4.1(2)	699(5)	400(5)	0.572(9)
2	5.083(2)	6.921(2)	154.9(2)	1.362	2.9(2)	719(5)	350(5)	0.487(8)

[a]Results obtained from Ref. 13.

solidified at room temperature in an epoxy resin in a field of 0.5 T that was applied parallel to the x-ray scattering vector.

The powder neutron diffraction experiments were performed at the Institut Laue Langevin in Grenoble, France on the D1B double-axis high-flux diffractometer which has a full width at half maximum resolution of 0.3°; a detailed description of D1B can be found[9] elsewhere. The samples were placed in 6 mm inner diameter cylindrical vanadium containers and the 2 and 295 K diffraction patterns were obtained over a 2θ angular range of 80° with a 400 cell ^{3}He detector that has a step of 0.2° between each cell. At 2 K a neutron wavelength of 2.52 Å, selected by a pyrolytic graphite monochromator, was used, whereas at 295 K, a neutron wavelength of 1.287 Å, as selected by the (311) Bragg reflection on a Ge monochromator with a take off angle of 44.2° in 2θ, was used. The powder diffraction patterns have been refined[9] with the FULLPROF suite of programs.

The Curie temperatures have been determined by using a Faraday balance and a heating and cooling rate of 5 K/min. Magnetization measurements have been performed by using the extraction method in a dc applied magnetic field of up to 9 T. The spontaneous magnetization, M_s, has been determined by extrapolation of the isothermal curve to zero applied field.

The Mössbauer spectra of $TbCo_3FeB$ and $TbCo_2Fe_2B$ have been measured between 85 and 295 K on a constant-acceleration spectrometer which utilized a rhodium matrix cobalt-57 source and was calibrated at room temperature with α-iron powder. The Mössbauer spectral absorbers contained 25 mg/cm^2 of powdered sample which had been sieved to a 0.050 mm or smaller diameter particle size.

III. STRUCTURAL ANALYSIS

The 295 K lattice parameters obtained from the powder x-ray diffraction patterns of the $TbCo_{4-x}Fe_xB$ compounds are given in Table I and their compositional dependence is shown in Fig. 1. Surprisingly, the a lattice parameter increases significantly between $x=0$ and 1 and then increases only slightly between $x=1$ and 2; in contrast the c lattice parameter decreases from $x=0$ to 1 and then increases substantially between $x=1$ and 2. This behavior indicates that a change in the substitutional pattern of cobalt by iron occurs at approximately $x=1$. A similar behavior has been observed for the $RCo_{4-x}Fe_xB$ compounds, where R is Y, Nd,[10,11] and Dy,[12] and results from the preferential substitution of cobalt by iron on the $2c$ crystallographic site. The combination of the anisotropic changes in lattice parameters with increasing x leads to an essentially linear increase in unit-cell volume, as shown in Fig. 1.

The substitutional replacement of cobalt by iron and the magnetic structure of $TbCo_3FeB$ and $TbCo_2Fe_2B$ have been determined from the neutron powder diffraction patterns obtained at 295 and 2 K, patterns that are shown in Fig. 2. The 2 K neutron diffraction pattern of $TbCo_3FeB$ indicates the clear presence of, at most, 5 wt % of a $Tb_3M_{11}B_4$ impurity, where M is Co and/or Fe; the neutron diffraction patterns of $TbCo_2Fe_2B$ reveal no impurities. The results of the 2 K refinement for $TbCo_3FeB$ and $TbCo_2Fe_2B$ are given in Table II

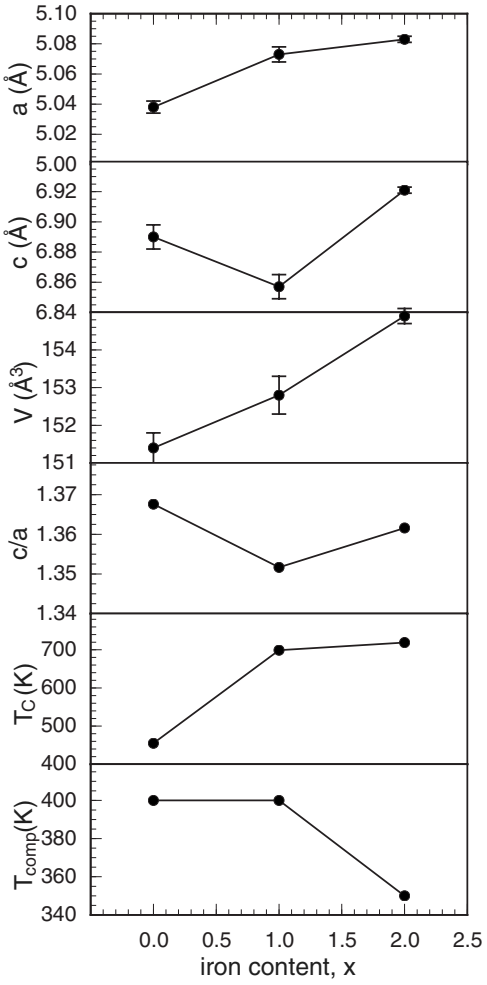

FIG. 1. The compositional dependence of the lattice parameters, the unit-cell volume, the c/a ratio, obtained from 295 K x-ray diffraction studies, and the Curie and compensation temperatures for the $TbCo_{4-x}Fe_xB$ compounds.

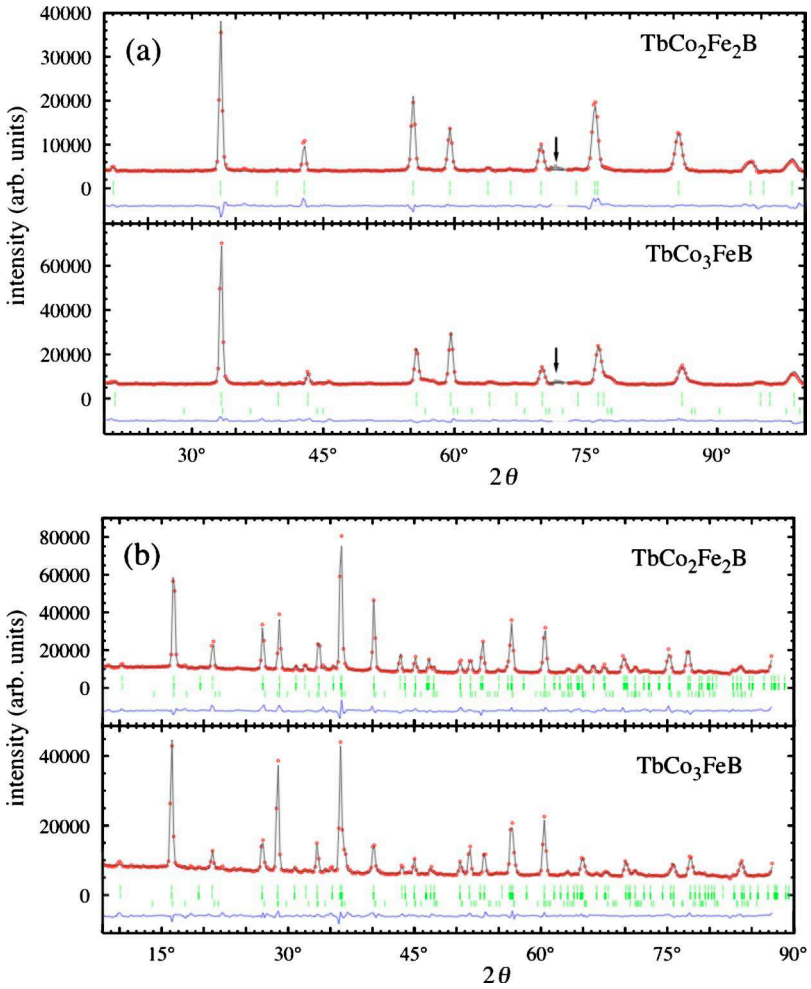

FIG. 2. (Color online) The powder neutron diffraction patterns of $TbCo_3FeB$ and $TbCo_2Fe_2B$ obtained at 2 K with a neutron wavelength of 2.52 Å (a) and at 290 K with a neutron wavelength of 1.287 Å (b). The red dots represent the experimental points; the black solid line represents the fit. From top to bottom, the green vertical bars represent the nuclear and magnetic diffraction peaks of the main phase and the diffraction peaks of the impurity. The residuals are plotted in blue. The arrow indicates the Bragg peak corresponding to the contribution from the vanadium tail of the cryostat.

together with the results obtained earlier[13] for $TbCo_4B$. The 2 K refinements indicate both a strong preferential occupation of the 2*c* site by iron with increasing *x* and a basal orientation of the magnetic moments. The 295 K neutron diffraction results confirm the strong preferential substitution of iron on the 2*c* site.

TABLE II. The 2 K neutron diffraction refinement results for $TbCo_{4-x}Fe_xB$.

x	0[a]	1	2
Instrument	D2B	D1B	D1B
a (Å)	5.035(1)	5.072(1)	5.080(1)
c (Å)	6.855(2)	6.841(1)	6.904(1)
z_{6i}/c	0.286(1)	0.261(7)	0.266(3)
Fe 2*c* occupancy (%)	⋯	72(6)	78(6)
Fe 6*i* occupancy (%)	⋯	12(4)	46(4)
μ_{Tb}^{1a} (μ_B)	8.0(7)	8.4(2)	7.8(2)
μ_{Tb}^{1b} (μ_B)	7.7(7)	8.7(3)	8.0(3)
μ_M^{2c} (μ_B)	1.6(2)	1.8(1)	1.7(1)
μ_M^{6i} (μ_B)	0.7(2)	0.8(1)	1.1(1)
χ^2	8.8	9.7	10.1
R_{Bragg} (%)	8.4	4.7	7.34
R_{mag} (%)	20.5	8.2	6.6
R_{wp} (%)	4.7	11.6	14.2
R_p (%)	2.5	15.5	18.1
R_{expt} (%)	3.3	3.7	4.5

[a]Results obtained from Ref. 13.

The terbium magnetic moments of approximately $8\mu_B$ observed in the $TbCo_{4-x}Fe_xB$ compounds are similar to the moments observed[14] in other terbium intermetallic compounds, such as the related $TbCo_4Ga$ and $TbCo_4Al$ compounds.[15] In contrast, the transition metal magnetic moments are small and different for the two sites, the 2*c* moment being larger than the 6*i* moment. In $TbCo_3FeB$ the transition metal magnetic moments are $1.8(1)\mu_B$ and $0.8(1)\mu_B$ on the 2*c* and 6*i* sites, respectively. These different values, which are very similar to those observed for $TbCo_4B$, indicate the importance of the 2*p*-3*d* orbital hybridization of the bonds between the boron and the cobalt, or the boron and iron, in reducing the 6*i* site magnetic moment. Further, the moment on the 6*i* site increases from $0.7\mu_B$ to $1.1\mu_B$ between $x=0$ and 2, an increase that likely results from a combination of the larger magnetic moment on iron than on cobalt and a smaller cobalt moment as a result of the increased distance between the cobalt 6*i* site and the boron 2*d* site, an increase that decreases the 2*p*-3*d* orbital hybridization of the boron-cobalt bond.

The 295 K x-ray diffraction patterns of the $TbCo_{4-x}Fe_xB$ compounds, with $x=0$, 1, and 2, oriented in an external magnetic field of 0.5 T, applied parallel to the x-ray scattering vector, show only the (*hk*0) Bragg peaks. Hence, at 295 K the easy magnetization direction is perpendicular to the crystallographic *c*-axis, i.e., the magnetization is basal.

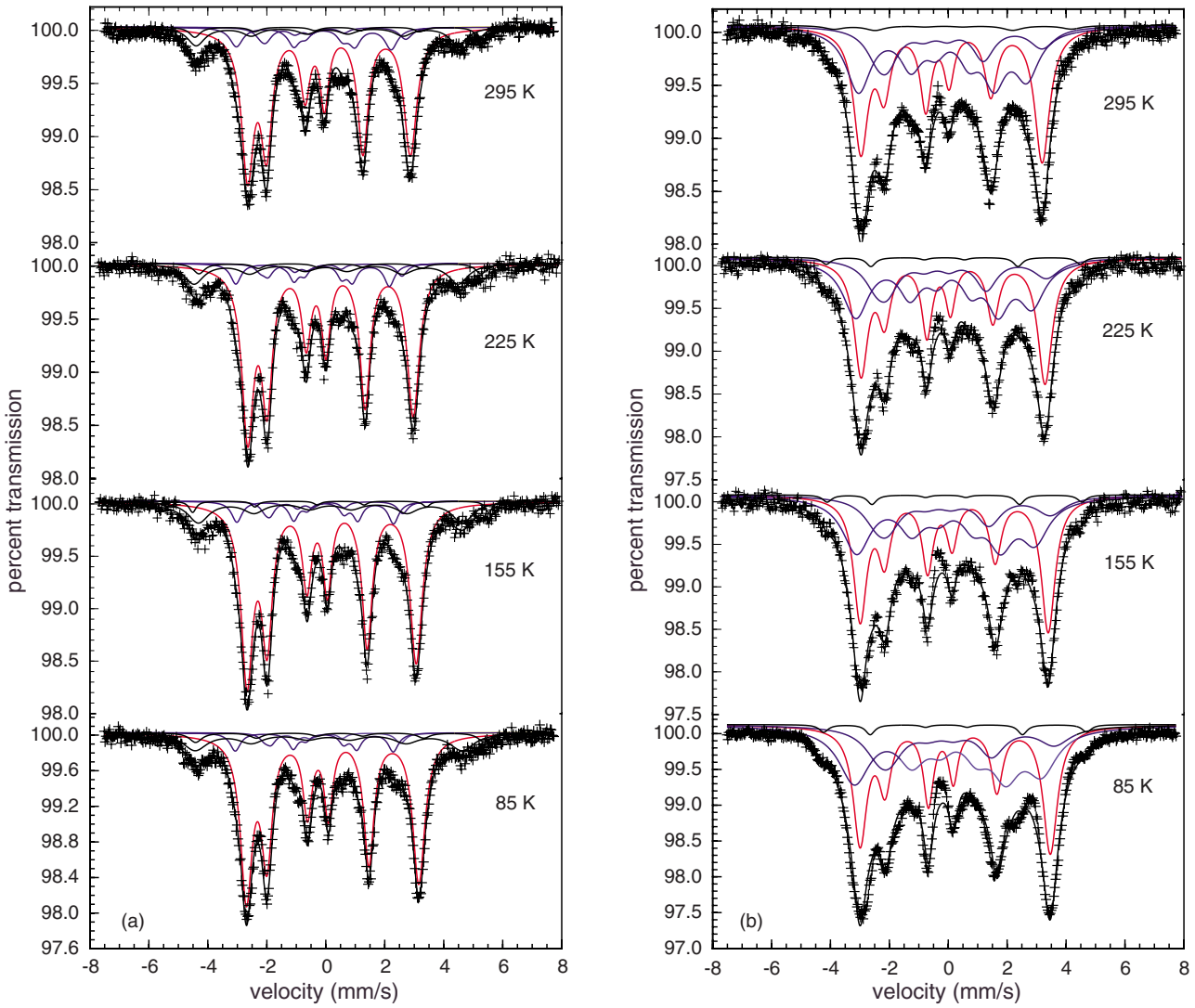

FIG. 3. (Color online) The Mössbauer spectra of $TbCo_3FeB$ (a) and $TbCo_2Fe_2B$ (b) obtained at the indicated temperatures. The red line and the two blue lines represent the 2*c* and 6*i* components to the total fit.

IV. MAGNETIC PROPERTIES

The Curie temperatures, T_C, of the $TbCo_{4-x}Fe_xB$ compounds, deduced from the thermomagnetic measurements, are given in Table I. The iron substitution from $x=0$ to 1 substantially increases the Curie temperature by 244 K from 455 to 699 K, whereas a further increase in x to 2 increases the Curie temperature by only 20 K up to 719 K. Similar increases in the Curie temperature have been reported for the isotypic $RCo_{4-x}Fe_xB$ compounds[10–12,16] and have been attributed, at least in part, to the increase in the transition metal sublattice magnetization and the concomitant unit-cell expansion.

The 4.2 K spontaneous magnetization decreases from $5.0\mu_B$ for $TbCo_4B$ to $2.9\mu_B$ for $TbCo_2Fe_2B$. This decrease results from an increase in the transition metal sublattice magnetic moment with increasing iron content, a sublattice moment that is antiparallel to that of the terbium sublattice. The compensation temperatures and their compositional dependency are given in Table I. The compensation temperature decreases with increasing iron content, in agreement with an increased transition metal sublattice magnetization and a constant terbium sublattice magnetization.

V. MÖSSBAUER SPECTRAL RESULTS

The Mössbauer spectra of $TbCo_3FeB$ and $TbCo_2Fe_2B$ obtained between 85 and 295 K are shown in Fig. 3. The Mössbauer spectra of $TbCo_3FeB$ exhibit the presence of 18(3)% by area of an iron containing impurity. The neutron diffraction pattern reveals the presence of at most 5 wt % of a $Tb_3M_{11}B_4$ impurity, a phase that is known[17,18] to accommodate a rather large amount of iron to form $Tb_3Co_{11-y}Fe_yB_4$. The 18% of iron impurity observed in the Mössbauer spectra corresponds to $y=5$, a rather large but not unreasonable amount[18] of iron in this impurity phase. The Mössbauer spectrum of $Y_3Co_{11-x}Fe_xB_4$ with $x=1.98$ observed earlier[17] but not analyzed in detail is very similar to both those observed[16] previously for the $YCo_{4-x}Fe_xB$ compounds and to that of $TbCo_3FeB$ reported herein. Hence, the comparison of the Mössbauer signal of the impurity in $TbCo_3FeB$ with the earlier spectrum of $Y_3Co_{11-x}Fe_xB_4$ is problematic and the nature of the impurity cannot be identi-

TABLE III. The Mössbauer spectral parameters for the $TbCo_{4-x}Fe_xB$ compounds. (The parameters are defined in the text and given with their statistical error limits if they have been refined.)

x	T (K)	Site	δ [a] (mm/s)	$e^2Qq/2$ (mm/s)	H (T)	η	θ (deg)	ϕ (deg)	% area	y	Γ (mm/s)	$\Delta\Gamma$
1	295	$2c$	−0.133(2)	−1.046(7)	16.59(1)	0	90	0	82(3)	1.34(3)	0.35(1)	0.06
		$6i_1$	−0.23(1)	1.25(3)	14.1(2)	1	0	90	6(1)		0.42(3)	0.04
		$6i_2$	−0.23(1)	1.25(3)	14.2(2)	1	120	90	12(1)		0.42(3)	0.04
	225	$2c$	−0.085(2)	−1.056(8)	16.86(2)	0	90	0	85(3)	1.40(4)	0.35(1)	0.05
		$6i_1$	−0.27(1)	1.32(4)	13.3(2)	1	0	90	5(1)		0.35(1)	0.03
		$6i_2$	−0.27(1)	1.32(4)	13.7(4)	1	120	90	10(1)		0.35(1)	0.03
	155	$2c$	−0.048(2)	−1.058(7)	17.26(2)	0	90	0	85(3)	1.54(4)	0.35(1)	0.05
		$6i_1$	−0.18(1)	1.19(3)	13.4(2)	1	0	90	5(1)		0.35(1)	0.03
		$6i_2$	−0.18(1)	1.19(3)	14.5(1)	1	120	90	10(1)		0.35(1)	0.03
	85	$2c$	−0.018(2)	−1.072(7)	17.60(2)	0	90	0	85(3)	1.60	0.35(1)	0.05
		$6i_1$	−0.21(1)	1.23(3)	12.9(2)	1	0	90	5(1)		0.46(7)	0.00
		$6i_2$	−0.21(1)	1.23(3)	14.5(1)	1	120	90	10(1)		0.46(7)	0.00
2	295	$2c$	−0.129(3)	−1.01(1)	18.66(3)	0	90	0	46(3)	4	0.419(8)	0.06
		$6i_1$	−0.022(9)	0.85(2)	17.2(1)	1	0	90	18(3)		0.78(2)	0.08
		$6i_2$	−0.022(9)	0.85(2)	16.8(1)	1	120	90	36(3)		0.78(2)	0.08
	225	$2c$	−0.083(3)	−1.04(1)	18.90(2)	0	90	0	43(1)	4	0.404(9)	0.06
		$6i_1$	0.02(1)	0.86(2)	17.9(1)	1	0	90	19(1)		0.82(3)	0.10
		$6i_2$	0.02(1)	0.86(2)	17.7(1)	1	120	90	38(1)		0.82(3)	0.10
	155	$2c$	−0.041(3)	−1.03(1)	19.36(2)	0	90	0	43(1)	4	0.43(1)	0.04
		$6i_1$	0.09(1)	0.88(2)	18.2(1)	1	0	90	19(1)		0.90(3)	0.08
		$6i_2$	0.09(1)	0.88(2)	17.9(1)	1	120	90	38(1)		0.90(3)	0.08
	85	$2c$	−0.007(1)	−1.024(6)	19.61(1)	0	90	0	40(2)	4	0.381(5)	0.06
		$6i$	0.175(6)	0.90(1)	18.48(7)	1	0	90	20(2)		0.94(2)	0.10
		$6i_2$	0.175(6)	0.90(1)	18.86(7)	1	120	90	40(2)		0.94(2)	0.10

[a]The isomer shifts are given relative to room temperature α-iron powder.

fied by its Mössbauer signature. Further, the spectra of $TbCo_2Fe_2B$ exhibit the presence of 2.0(5)% by area of an impurity whose hyperfine fields are compatible with those of an FeCo alloy impurity, an amount of impurity probably too small to be observed by neutron diffraction.

A comparison of the spectra of $TbCo_3FeB$ and $TbCo_2Fe_2B$ with those of the other $RCo_{4-x}Fe_xB$ compounds,[12,16,19] where R is Y, Gd, and Dy, indicates that the magnetization and, hence, the iron magnetic moments and hyperfine fields are oriented in the basal plane of the hexagonal unit cell, a conclusion that agrees with the conclusion drawn from the oriented powder x-ray diffraction and neutron diffraction results.

Because iron is present on both the $2c$ and $6i$ sites in the structures of $TbCo_3FeB$ and $TbCo_2Fe_2B$, at least two contributions are required to fit their Mössbauer spectra. Further, both because of the basal orientation of the iron magnetic moments and hence hyperfine fields and because of the $6i$ point symmetry, the $6i$ contribution must be subdivided[16,19] into two components with relative areas of 1:2, see below. In preliminary fits the relative areas of the $2c$ and $6i$ contributions have been constrained to the iron occupancies obtained from neutron diffraction studies; in the final fits shown in Fig. 3 they have been refined.

The simultaneous presence of both small hyperfine fields and large quadrupole interactions in the iron-57 Mössbauer spectra of $TbCo_3FeB$ and $TbCo_2Fe_2B$ prevents their analysis with a first-order perturbation of the Zeeman magnetic Hamiltonian by the quadrupole interaction. Rather, an exact solution for both the iron-57 ground and excited state Hamiltonians must be used to fit the spectra. The resulting fits are shown as the lines and spectral components in Fig. 3; the corresponding spectral parameters with their statistical errors are given in Table III. The actual errors are probably twice as large as the statistical errors.

In agreement with the point symmetry of the $2c$ and $6i$ sites[20] and the basal orientation of the iron magnetic moments, the asymmetry parameter and the Euler angles, θ and ϕ, of the hyperfine field in the electric field gradient axes have been fixed to the values already obtained[12] for $DyCo_{4-x}Fe_xB$ and given in Table III. The isomer shift, δ, the hyperfine field, H, and the quadrupole interaction, $e^2Qq/2$, for both the $2c$ and $6i$ sites have been adjusted.

In addition to adjusting the above hyperfine parameters and the line width, Γ, an incremental line width, $\Delta\Gamma$, defined as $\Gamma(v)=\Gamma+(v-\delta)\Delta\Gamma$, where v is the velocity and δ is the isomer shift of a given spectral component, has also been

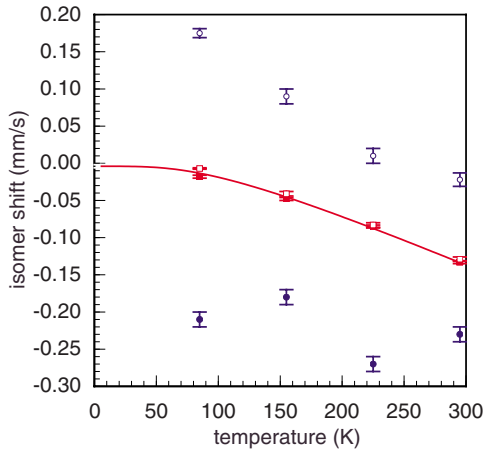

FIG. 4. (Color online) The temperature dependence of the 2*c*, red symbols, and 6*i*, blue symbols, and isomer shifts in $TbCo_3FeB$, closed symbols, and $TbCo_2Fe_2B$, open symbols. The red solid line is a fit with the Debye model for the 2*c* isomer shifts.

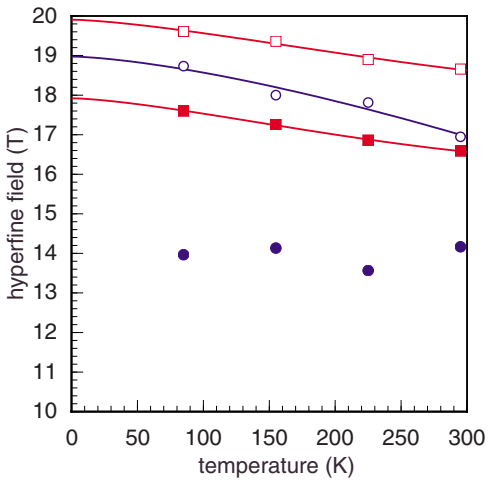

FIG. 5. (Color online) The temperature dependence of the 2*c*, red squares, and 6*i*, blue circles, and hyperfine fields in $TbCo_3FeB$, closed symbols, and $TbCo_2Fe_2B$, open symbols.

fitted in order to account for the distribution of cobalt and iron on the near neighbors of the 2*c* and 6*i* sites. Finally, a texture parameter, *y*, has been introduced into the fits as a factor multiplying the Clebsch–Gordan coefficient of the $\Delta m=0$ transitions. In the case of a sextet this is essentially equivalent to a component area ratio of $3:y:1:1:y:3$, where *y* may vary from zero for a hyperfine field parallel to the γ-ray direction to 4 for a hyperfine field perpendicular to the γ-ray direction. The relative areas of the 2*c* and 6*i* components have been adjusted starting from the initial values given by the iron occupancies obtained from the neutron powder diffraction patterns of $TbCo_3FeB$ and $TbCo_2Fe_2B$.

Under the assumption that the recoil free fractions of the two iron sites are equal, the refined temperature independent relative areas of the 2*c* and 6*i* sites are in reasonable agreement with the site occupancies obtained from the neutron diffraction measurements and given in Table II.

The temperature dependence of the 2*c* and 6*i* isomer shifts in $TbCo_3FeB$ and $TbCo_2Fe_2B$ is shown in Fig. 4 and, in the absence of any change in the structure or in the iron electronic configuration, the observed temperature dependence results from a combination of both lattice expansion and the second-order Doppler shift. Because the lattice expansion would favor an increase in the isomer shift with increasing temperature, the observed decrease in the isomer shift with increasing temperature results primarily from the second-order Doppler shift. The temperature dependence of the 2*c* isomer shift, which is better defined because of the higher iron occupancy of this site, has been fitted with the Debye model[21] for the second-order Doppler shift, and an identical Mössbauer lattice temperature of 375(27) K was obtained for both $TbCo_3FeB$ and $TbCo_2Fe_2B$. This value falls within the range of 265–410 K observed[22] for several R_2Fe_{17} compounds and is similar to the value of 447(75) K observed[23] in $YCoFe_3B$. The 2*c* isomer shift is essentially independent of *x* whereas the 6*i* isomer shift increases with increasing *x* in a fashion similar to that observed[12] in the $DyCo_{4-x}Fe_xB$ compounds. This increase in the 6*i* isomer shift may result from the increase in the *c* lattice parameter and in the unit-cell volume in going from $TbCo_3FeB$ to $TbCo_2Fe_2B$. The quadrupole interactions of both the 2*c* and 6*i* sites are independent of temperature. The 2*c* quadrupole interaction is independent of *x*, whereas the 6*i* quadrupole interaction decreases upon going from $TbCo_3FeB$ to $TbCo_2Fe_2B$.

Both the 2*c* and 6*i* hyperfine fields increase with increasing iron content, in agreement with the increase in the transition metal sublattice magnetization. The relatively small hyperfine fields of between 13 and 20 T observed for both sites result from a combination of the Fermi contact and orbital contributions to the hyperfine field, contributions that have been discussed earlier.[16,19] As previously observed for the $RCo_{4-x}Fe_xB$ compounds,[12,16,19,20] where *R* is Y, Pr, Nd, Sm, Gd, and Dy, the 2*c* hyperfine field is larger than the weighted average 6*i* hyperfine field, in agreement with the larger transition metal magnetic moment obtained from the neutron diffraction patterns, see Table II.

The temperature dependence of the 2*c* and average 6*i* hyperfine fields in $TbCo_3FeB$ and $TbCo_2Fe_2B$ is shown in Fig. 5. As expected the hyperfine fields decrease with increasing temperature, with the exception of the average 6*i* hyperfine field in $TbCo_3FeB$, which is poorly determined because of the small iron occupancy of this site. The solid lines shown in Fig. 5 are the result of a least-squares fit[24] with the equation

$$B = B_0[1 - C_{3/2}(T/T_C)^{3/2} - C_{5/2}(T/T_C)^{5/2}],$$

where B_0 and T_C are the saturation field and Curie temperature, respectively. The Curie temperatures given in Table I were used in the fit. The $C_{3/2}$ coefficients are equal to 0.47, 0.37, and 0.42 and $C_{5/2}$ are equal to −0.46, −0.33, and −0.06 for the 2*c* site in $TbCo_3FeB$ and the 2*c* and 6*i* sites in $TbCo_2Fe_2B$, respectively.

VI. DISCUSSION AND CONCLUSIONS

The iron occupancies determined from neutron diffraction and the relative areas of the three contributions to the Mössbauer spectra of the $TbCo_{4-x}Fe_xB$ compounds indicate that iron preferentially substitutes for cobalt on the 2*c* crys-

tallographic site. This preferential substitution explains the observed compositional dependence of the lattice parameters, a dependence that takes place in two steps, first, between $x=0$ and 1 and, second, for x greater than 1. A higher iron content increases the transition metal sublattice magnetization and consequently decreases the compensation temperature. The ordering temperature strongly increases from 455 to 719 K between $x=0$ and 2. The large increase in ordering temperature from $x=0$ to 1 results almost exclusively from the preferential substitution of cobalt by iron on the 2*c* site. Hence, the exchange interactions in the $R\mathrm{Co}_{4-x}\mathrm{Fe}_x\mathrm{B}$ compounds are largely determined by the transition metal 2*c* site. The dominant magnetic role of the 2*c* site is also apparent in its larger hyperfine field observed in the Mössbauer spectra, a larger field that is associated with a larger magnetic moment. Both iron and cobalt exhibit a larger 2*c* than 6*i* magnetic moment because of the strong hybridization between their 3*d* orbital and the near-neighbor boron 2*p* orbital.

ACKNOWLEDGMENTS

The authors are grateful to Dr. Raphaël P. Hermann for his help in developing the code to analyze the Mössbauer spectra and to Dr. M. Sougrati for his help in the Mössbauer laboratory. This work was partially supported by the Fonds National de la Recherche Scientifique, Belgium through Grant Nos. 9.456595 and 1.5.064.05, by the "Commissariat Général aux Relations Internationales, Ministère de la Communauté Française de Belgique, Relations scientifiques avec la France," Grant No. 2007/02242/S, and by the CNRS-Cooperation Program, Contract No. PVB/ADK/FR/0084-22/03/2006-091-S.

[1] J. F. Herbst, Rev. Mod. Phys. **63**, 819 (1991).
[2] Y. B. Kuz'ma and N. S. Bilonizhko, Sov. Phys. Crystallogr. **18**, 447 (1974).
[3] Y. B. Kuz'ma, N. S. Bilonizhko, S. I. Mykhalenko, G. F. Stepanova, and N. F. Chaban, J. Less-Common Met. **67**, 51 (1979).
[4] C. Zlotea, C. Chacon, and O. Isnard, J. Appl. Phys. **92**, 7382 (2002).
[5] C. Chacon and O. Isnard, J. Phys.: Condens. Matter **13**, 5841 (2001).
[6] C. Kaiser, A. F. Pachula, and S. S. P. Parkin, Phys. Rev. Lett. **95**, 047202 (2005).
[7] C. Chacon and O. Isnard, J. Solid State Chem. **154**, 242 (2000).
[8] E. N. Caspi, H. Pinto, and M. Melamud, J. Appl. Phys. **87**, 416 (2000).
[9] J. Rodriguez-Carvajal, Physica B **192**, 55 (1993).
[10] C. Chacon and O. Isnard, J. Appl. Phys. **89**, 71 (2001).
[11] O. Isnard and C. Chacon Carillo, J. Alloys Compd. **442**, 22 (2007).
[12] H. Mayot, O. Isnard, F. Grandjean, and G. J. Long, J. Appl. Phys. **103**, 093917 (2008).
[13] C. Chacon, Ph.D. thesis, Université Joseph Fourier-Grenoble I, 2000.
[14] E. du Trémolet de Lacheisserie, *Magnétisme* (Edition de Physique, Sciences, Paris, 2000), Vol. I.
[15] C. Zlotea and O. Isnard, J. Phys.: Condens. Matter **14**, 10211 (2002).
[16] G. J. Long, R. P. Hermann, F. Grandjean, C. Chacon, and O. Isnard, J. Phys.: Condens. Matter **18**, 10765 (2006).
[17] C. V. Thang, J. Stanek, P. E. Brommer, N. M. Hong, J. J. M. Franse, and N. P. Thuy, J. Magn. Magn. Mater. **157–158**, 645 (1996).
[18] N. Plugaru, M. Valeanu, D. L. Lazar, D. Matulescu, J. Wang, N. Tang, and F. M. Yang, J. Magn. Magn. Mater. **157–158**, 647 (1996).
[19] F. Grandjean, R. P. Hermann, E. Popiel, and G. J. Long, J. Appl. Phys. **101**, 023917 (2007).
[20] Y. Gros, F. Hartmann-Boutron, C. Meyer, M. A. Fremy, and P. Tenaud, J. Magn. Magn. Mater. **74**, 319 (1988).
[21] G. K. Shenoy, F. E. Wagner, and G. M. Kalvius, in *Mössbauer Isomer Shifts*, edited by G. K. Shenoy and F. E. Wagner (North-Holland, Amsterdam, 1978), p. 49.
[22] G. J. Long, O. Isnard, and F. Grandjean, J. Appl. Phys. **91**, 1423 (2002).
[23] F. Grandjean, M. T. Sougrati, H. Mayot, O. Isnard, and G. J. Long, J. Phys.: Condens. Matter **21** 186001 (2009).
[24] H. N. Ok, K. S. Baek, and C. S. Kim, Phys. Rev. B **24**, 6600 (1981).